Measuring the Reliability of Geometries in Magnet Resonance Angiography

A Reference for Multimodal Image Registration?

M. André Gaudnek[1,2], Andreas Hess[2,3], Klaus Obermayer[1,2], Michael Sibila[1,2]

[1]University of Technology, Neural Information Processing Group, Berlin, Germany
[2]Bernstein Centre for Computational Neuroscience, Berlin, Germany
[3]Institute for Experimental and Clinical Pharmacology,
University Erlangen-Nuremburg, Erlangen, Germany
grenjen@cs.tu-berlin.de

Abstract. Magnet Resonance Angiography (MRA) can be used to register MR images of other types (e.g. functional MRI) acquired in the same imaging session as the angiogram since blood vessels are spatially closely confined features. This is only possible if MRA delivers reliable, reproducible images and does not show major random distortions. Therefore, we examine the reliability of MRA over subsequent scanning sessions using an appropriate distance measure on geometric vasculature models obtained from MR angiograms. Additionally we examine the variance between different specimens in order to value the possibility of inter-specimen registration.

1 Introduction

Several applications of MR small animal brain image analysis like the generation of generic functional atlases or the combination of functional data from different modalities [1] rely on the comparison and combination of numerous images of the same or distinct specimens. In this context cerebral vascular MR angiograms play an important role as blood vessels can be used as excellent landmarks for image registration. On the one hand from this application arises the need for reliable, spatially correct angiograms, on the other hand MR images are known to be prone to local distortions. When it comes to the comparison of images from different specimens, additional variability is expected due to the natural variance between each individual's anatomic characteristic.

In order to inspect the spatial reliability of MR angiograms for different MR sequences as well as the cerebral vascular variability between different animals, we use a distance measure that is defined on a geometric model representation of vasculatures.

2 Materials and Methods

All MR angiograms are converted into geometrical representations of the vascular system using an automatic reconstruction algorithm [2]. In these models vessels

are represented as chains of connected frustums. The distance measure we use to evaluate the similarity of two distinct vascular models mainly calculates the mean distance between nearest frustum center line segments.

If A, B are two vascular models, then for each frustum a of A the distance $d_{fr}(a)$ is defined as the smallest centerline-to-centerline distance $d_{\text{cen}}(a, b)$ between any point of the center line segment of a and any point of any center line segment in B, i.e.

$$d_{fr}(a) = \min_{b \in B} d_{\text{cen}}(a, b) \tag{1}$$

The distance $d_{\text{mod}}(A, B)$ between both models is then calculated as the mean of the distances of all segments of A to B:

$$d_{\text{mod}}(A, B) = \langle d_{fr}(a) \rangle_{a \in A} \tag{2}$$

This measure is not commutative, i.e. usually $d_{\text{mod}}(A, B) \neq d_{\text{mod}}(B, A)$, but in practice only slight differences should occur.

The calculation of $d_{\text{cen}}(a, b)$ needs only basic mathematics and a couple of case differentiations. The center line segments c_a and c_b of a and b can be expressed using line equations with restricted independent variables t_a and t_b:

$$c_a = \{\boldsymbol{s}_a + t_a \boldsymbol{m}_a | 0 \leq t_a \leq 1, \boldsymbol{m}_a = \boldsymbol{e}_a - \boldsymbol{s}_a\} \tag{3}$$

$$c_b = \{\boldsymbol{s}_b + t_b \boldsymbol{m}_b | 0 \leq t_b \leq 1, \boldsymbol{m}_b = \boldsymbol{e}_b - \boldsymbol{s}_b\} \tag{4}$$

where $\boldsymbol{s}_a$, $\boldsymbol{s}_b$ are the segment starting points and $\boldsymbol{e}_a$, $\boldsymbol{e}_b$ are the segment ending points. There are five distance calculation cases that have to be distinguished, 2 for parallel segments and 3 for non-parallel segments (Fig. 2).

If the segments are parallel, we build two perpendiculars from $\boldsymbol{s}_b$ and $\boldsymbol{e}_b$ onto c_a. This results in two base points $\boldsymbol{p}_s$ and $\boldsymbol{p}_e$ which can also be expressed by specific values for t_a. As the line through $\boldsymbol{s}_b$ and $\boldsymbol{p}_s$ is orthogonal to $\boldsymbol{m}_b$, following equation holds:

$$0 = (\boldsymbol{p}_s - \boldsymbol{s}_b) \cdot \boldsymbol{m}_b \tag{5}$$

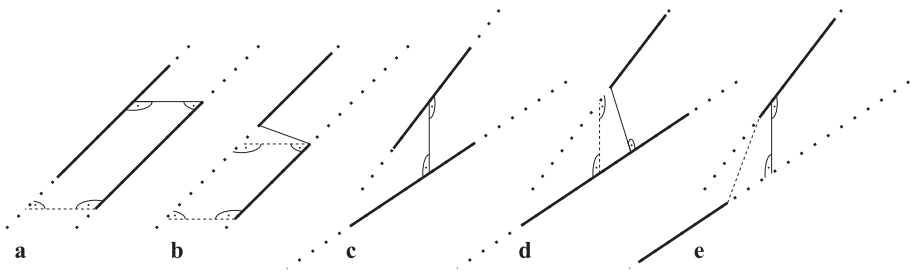

Fig. 1. All segment-to-segment distance calculation cases. Thick solid lines are center line segments, thin solid lines the smallest distance vectors: Segemnts are parallel overlapping (a); parallel non-overlapping (b), non-parallel overlapping (c), non-parallel non-overlapping with smallest distance between endpoint and line segment (d) and with smallest distance between endpoints (e)

$\boldsymbol{p}_s$ is on the line defined in (3), so

$$0 = (\boldsymbol{s}_a + t_{a,ps}\boldsymbol{m}_a - \boldsymbol{s}_b) \cdot \boldsymbol{m}_b \Longleftrightarrow t_{a,ps} = \frac{(\boldsymbol{s}_b - \boldsymbol{s}_a) \cdot \boldsymbol{m}_b}{\boldsymbol{m}_a \cdot \boldsymbol{m}_b} \tag{6}$$

$t_{a,pe}$ is calculated analogically. If $t_{a,pe}, t_{a,ps} < 0$, segment b is completely left of segment a, if $t_{a,pe}, t_{a,ps} > 1$, segment b is completely right of segment a. In both cases the smallest distance $d_{\text{cen}}(a, b)$ between both segments is found between a pair of their end points (Fig. 2b), i.e.

$$d_{\text{cen}}(a, b) = \min\{\|\boldsymbol{s}_b - \boldsymbol{s}_a\|, \|\boldsymbol{s}_b - \boldsymbol{e}_a\|, \|\boldsymbol{e}_b - \boldsymbol{s}_a\|, \|\boldsymbol{e}_b - \boldsymbol{e}_a\|\} \tag{7}$$

In all other cases, there are actually overlapping parts of c_a and c_b, and $d_{\text{cen}}(a, b)$ can be calculated as the distance between $\boldsymbol{s}_b$ and $\boldsymbol{p}_s$ (Fig. 2a):

$$d_{\text{cen}}(a, b) = \|\boldsymbol{s}_a + t_{a,ps}\boldsymbol{m}_a - \boldsymbol{s}_b\| \tag{8}$$

3 Results

If the segments are not parallel, first a normalized vector orthogonal to both lines is constructed as

$$\boldsymbol{n} = \frac{\boldsymbol{m}_a \times \boldsymbol{m}_b}{\|\boldsymbol{m}_a \times \boldsymbol{m}_b\|} \tag{9}$$

$\boldsymbol{n}$ is directed along the shortest perpendicular between both lines, the line-to-line distance $\tilde{d}$ as well as the base point parameters $t_{a,p}$ and $t_{b,p}$ are calculated by solving the linear equation

$$\boldsymbol{s}_a + t_{a,p}\boldsymbol{m}_a + \tilde{d}\boldsymbol{n} = \boldsymbol{s}_b + t_{b,p}\boldsymbol{m}_b \tag{10}$$

If $0 \leq t_{a,p}, t_{b,p} \leq 1$, both base points are actually located on the line segments and the distance is

$$d_{\text{cen}}(a, b) = |\tilde{d}| \tag{11}$$

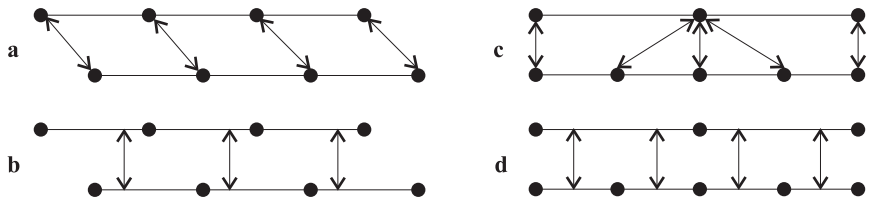

Fig. 2. Shifted segment end points lead to an overestimation when using point-to-point distance (a), whereas the distance is measured correctly using segment-to-segment distance (b). Different point density also leads to distance overestimation with point-to-point distance (c), segment-to-segment distance leads to correct results (d)

If one of the t-values is outside the range [0..1], the shortest distance could be found along a perpendicular from one of the four segment end points onto the corresponding counter-line (Fig. 2d). The t-values for the four perpendiculars are calculated

$$\begin{aligned} t_{a,sb} &= \frac{(\boldsymbol{s}_b - \boldsymbol{s}_a)\cdot \boldsymbol{m}_a}{\|\boldsymbol{m}_a\|^2}, t_{a,eb} = \frac{(\boldsymbol{e}_b - \boldsymbol{s}_a)\cdot \boldsymbol{m}_a}{\|\boldsymbol{m}_a\|^2} \\ t_{b,sa} &= \frac{(\boldsymbol{s}_a - \boldsymbol{s}_b)\cdot \boldsymbol{m}_b}{\|\boldsymbol{m}_b\|^2}, t_{b,ea} = \frac{(\boldsymbol{e}_a - \boldsymbol{s}_b)\cdot \boldsymbol{m}_b}{\|\boldsymbol{m}_b\|^2} \end{aligned} \tag{12}$$

For every t-value in the range [0..1] the corresponding distance can be calculated

$$\begin{aligned} \tilde{d}_{a,sb} &= \|\boldsymbol{s}_a + t_{a,sb}\boldsymbol{m}_a - \boldsymbol{s}_b\|, \tilde{d}_{a,eb} = \|\boldsymbol{s}_a + t_{a,eb}\boldsymbol{m}_a - \boldsymbol{e}_b\| \\ \tilde{d}_{b,sa} &= \|\boldsymbol{s}_b + t_{b,sa}\boldsymbol{m}_b - \boldsymbol{s}_a\|, \tilde{d}_{b,ea} = \|\boldsymbol{s}_b + t_{b,ea}\boldsymbol{m}_b - \boldsymbol{e}_a\| \end{aligned} \tag{13}$$

If none of the t-values is in the valid range, the case shown in fig. 2e applies and the distance is again determined by the smallest distance between an endpoint pair and calculated as in (7). Vessels present in model A but not in model B lead to an overestimation of the mean distance, as their nearest counterpart in B belongs to a different, distant part of the vasculature. Therefore, distances are pruned above an adjustable threshold.

Although more complex and time consuming to calculate, this measure has two major advantages over one that is based on the calculation of minimal distances between centerline segment end points only (Fig. 2):

- It is independent of the end point densities in both models, they may differ considerably.
- Calculation based on end points is prone to bias with specific shifts, which cannot occur using line-to-line distances.

However, the effects are not as drastic as the theoretical reasoning for using the new distance measure induces since the high number of points in our models smoothes the expected strong discontinuities (Fig. 3).

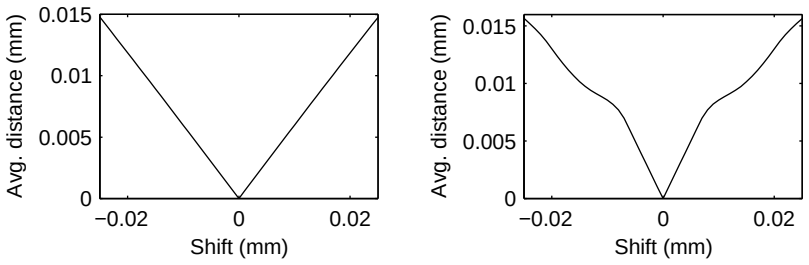

Fig. 3. Measured distance of a vascular system model with 1466 points shifted against a copy of it along one spatial axis. Left: The measure as described in this paper reveals a linear correlation between shift and distance. Right: A simple measure solely based on point-to-point distances results a comparably distorted correlation between shift and measured distance

Table 1. Mean distance and variance in μm between vascular system reconstructions from the same rat but different days (FU1-FU4) and different rats (H156-H341)

	FU1	FU2	FU3	FU4	H156	H209	H316	H341
FU1		10.12 ± 0.18	11.46 ± 0.19	10.41 ± 0.14	27.55 ± 0.28	27.73 ± 0.29	28.74 ± 0.32	27.42 ± 0.24
FU2	7.49 ± 0.10		9.04 ± 0.09	8.24 ± 0.07	25.90 ± 0.27	27.17 ± 0.26	26.02 ± 0.26	26.67 ± 0.22
FU3	8.51 ± 0.10	10.65 ± 0.15		9.67 ± 0.14	28.06 ± 0.28	27.85 ± 0.28	25.79 ± 0.29	26.99 ± 0.24
FU4	10.19 ± 0.14	10.87 ± 0.17	9.91 ± 0.16		27.62 ± 0.30	27.82 ± 0.27	26.36 ± 0.28	28.10 ± 0.24
H156	28.62 ± 0.31	28.93 ± 0.35	30.36 ± 0.32	28.13 ± 0.30		28.90 ± 0.30	29.90 ± 0.35	28.21 ± 0.26
H209	26.30 ± 0.28	26.93 ± 0.27	28.07 ± 0.30	27.04 ± 0.27	26.32 ± 0.26		26.53 ± 0.27	25.72 ± 0.24
H316	28.93 ± 0.35	29.58 ± 0.33	29.28 ± 0.36	27.98 ± 0.32	29.47 ± 0.32	28.42 ± 0.31		27.47 ± 0.26
H341	28.17 ± 0.25	28.69 ± 0.24	29.09 ± 0.28	28.90 ± 0.25	28.22 ± 0.24	28.08 ± 0.29	27.10 ± 0.28	

The inspection of 3D TOF scans of the same specimens on subsequent days reveals variances which reside in the range of the scan resolution, no significant distortions are found. 3D TOF scans of distinct specimens reveal considerably higher distances, so it is easy to discriminate using the distance value whether two scans of the same or of different animals are compared (table 1). In general the variance between different animals is smaller for the central brain areas. Although PCA and especially 2D TOF image a different subset of the whole vasculature, common parts are still well aligned.

4 Discussion

Our present results indicate that local MR distortions are of no concern for the vasculature-based registration of MR images. The registration of images from different scan sessions of the same specimen in order to compensate deviating head positions should be possible with high precision in the range of the resolution while the alignment transform for an angiogram obtained in the same session can be used to align functional images.

As the variance of the cerebral vasculature between different animals seems to be acceptable small, it could be possible to generate a digital atlas that encodes mean position and variance of at least the major brain blood vessels, thus subsequently allowing automatic vessel labeling.

The combination of MR angiograms with optical imaging is subject of our current experiments. Assuming OI to deliver as stable imaging as MRA, it should be possible to use 2D projections of vascular models to register MR images with optical images.

References

1. Hess A, Stiller D, Kaulisch T, et al. New insights into the hemodynamic blood oxygenation level-dependent response through combination of functional MRI and optical recording in gerbil barrel cortex. J Neurosci. 2000;20(9):3328–38.
2. Gaudnek M, Hess A, Obermayer K, et al. Geometric reconstruction of the rat vascular system imaged by MRA. Proc IEEE ICIP. 2005; p. 1278–81.